

# Catalytic hydrolysis of CFC-12 over $\text{MoO}_3/\text{ZrO}_2\text{-TiO}_2$ solid acid

**Zhiqian Li**

Yunnan Minzu University

**Tong Zhou**

Dehong Teachers College

**Guoqing Ren**

Yunnan Minzu University

**Xiaofang Tan**

Yunnan Minzu University

**Lijuan Jia**

Yunnan Minzu University

**Tiancheng Liu** (✉ [liutiancheng76@163.com](mailto:liutiancheng76@163.com))

College of Chemistry and Environment, Yunnan Minzu University, Joint Research Centre for International Cross-border Ethnic Regions Biomass Clean Utilization in Yunnan, Kunming 650500, China

---

## Research article

**Keywords:** Difluorodichloromethane(CFC-12), Chlorofluorocarbons(CFCs), Solid acids, Catalytic hydrolysis,  $\text{MoO}_3/\text{ZrO}_2\text{-TiO}_2$

**Posted Date:** October 15th, 2020

**DOI:** <https://doi.org/10.21203/rs.2.19505/v5>

**License:**   This work is licensed under a Creative Commons Attribution 4.0 International License.

[Read Full License](#)

---

# Abstract

The catalytic hydrolysis of Difluorodichloromethane(CFC-12) by solid acid of  $\text{MoO}_3/\text{ZrO}_2\text{-TiO}_2$  calcined at different temperature had been studied. The effects of catalytic hydrolysis temperature and water vapor concentration on catalytic hydrolysis of CFC-12 were also studied. The results showed that catalytic hydrolysis rate of CFC-12 reached to 98.65% at 400 °C when the  $\text{MoO}_3/\text{ZrO}_2\text{-TiO}_2$  catalyst was calcined at 500 °C with a concentration of water vapor of 83.18%, and the main hydrolysis products were CO,  $\text{CO}_2$ , HF and HCl. After 30 hours' continuous reaction, the hydrolysis rate of CFC-12 was 65.34%. The XRD result reveals that the main phase of solid  $\text{MoO}_3/\text{ZrO}_2\text{-TiO}_2$  catalyst is the tetragonal  $\text{Zr}(\text{MoO}_4)_2$  with doped  $\text{TiO}_2$  of anatase.

## Introduction

Chlorofluorocarbons (CFCs) have been broadly utilized in chemical industry due to their superior physical and chemical properties. However, more and more research showed that CFCs is harmful for ozone layer. Molina and Rowland proved that CFCs are a killer of ozone layer that protects humans against harmful ultraviolet radiation from the sun in 1974[1, 2]. Moreover, CFCs as green house gases have a great negative impact on human health and ecological environment. The research of CFCs has recently attracted many experts and scholars all over the world [3]. For example, in 1985, the Vienna Convention was established to restrict the use of CFCs for protecting the ozone layer, facilitated by United Nations Environment Program. With the enhancement of environmental awareness, 46 countries signed the Montreal Protocol (hereinafter referred to as protocol) in Montreal, Canada in 1987. Over time, the United Nation organized several meetings again, strengthen efforts that limited use of CFCs, modified protocol clearly stipulates that developing countries to stop using CFCs, CFCB,  $\text{CCl}_4$ ,  $\text{CH}_3\text{CCl}_3$ .

So far, the technology of harmless treatment of chlorofluorocarbons mainly includes chemical method, incineration, cement kiln, induction plasma, supercritical water and photocatalysis, etc [4-7]. However this methods have some limitations, therefore, it is urgent to pursue safe and efficient method of hydrolysis of CFCs. Solid super acid [8-11] is one of the new catalytic materials that has developed rapidly in recent years. The solid super acid catalytic has advantage of excellent catalytic activity, pollution-free, stability and reusability, thus this type of materials also become very popular in catalytic hydrolysis of CFC-12[12-14]. The catalytic performance of  $\text{MoO}_3/\text{ZrO}_2\text{-TiO}_2$  solid acid catalysts calcined at different temperatures for the hydrolysis of CFC-12 was studied, including the catalyst life. The effects of hydrolysis temperature and steam concentration on the reaction were also investigated[15-17]. The conditions of catalytic hydrolysis of CFC-12[18-20] were optimized, which provided a theoretical basis for a large number of harmless treatment of CFC-12.

## Experimental

### Catalyst preparation

The MoO<sub>3</sub>/TiO<sub>2</sub>-ZrO<sub>2</sub> catalyst were prepared by a wetness impregnation. Firstly, 5 ml TiCl<sub>4</sub> solution was added into 30 ml absolute ethyl alcohol solution in ice bath conditions. Then 6.2968 g ZrOCl<sub>2</sub>·8H<sub>2</sub>O was dissolved in mother solution. Secondly, the pH was adjusted to 8 with 10% ammonia, then took out the solid, washed out the Cl<sup>-</sup> with deionized water and dried it at 110 °C. Next, the precursor was impregnated in 0.25 mol/L (NH<sub>4</sub>)<sub>6</sub>MoO<sub>24</sub>·4H<sub>2</sub>O at 60 °C for 6 hours. Finally, the impregnation liquid was filtered, dried at 110 °C and calcined at a certain temperature for 3 hours.

### **Catalyst characterization**

In order to understand the morphology of catalyst, this paper has taken the following characterization tools. Firstly, the surface composition of the catalysts is analyzed by X-ray, the instruments are produced in Germany, the model is BRUKER D8ADVANCE. Secondly, the surface morphology of catalysts is analyzed by scanning electron microscopy with spectrum analyzer, the equipment is produced by FEI company of United States, its model is NOVA NANOSEM-450. The crystal structure of the catalyst was analyzed by transmission electron microscope, the equipment was produced by Japan Electronics Company, model JEM2106. BET N<sub>2</sub> isotherm adsorption desorption was used to determine the specific surface area and pore distribution of the catalyst, the equipment was produced by Macchik Bayer company, its model is BELSORP - max.

## **Catalyst experiment**

The catalyst hydrolysis test was performed in a fixed bed reactor at one atmospheric pressure. 1.00 g of catalyst (MoO<sub>3</sub>/TiO<sub>2</sub>-ZrO<sub>2</sub>) and 50 g SiO<sub>2</sub> were added into quartz tubes (Φ30×700 mm). A mixed gas stream of CFC-12, H<sub>2</sub>O(g), O<sub>2</sub> and He was introduced into the reactor with a total flow rate of 15 ml/min. The catalytic performance of MoO<sub>3</sub>/ZrO<sub>2</sub>-TiO<sub>2</sub> solid acid catalyst calcined at different temperature for the catalytic hydrolysis of CFC-12 was investigated. The effects of hydrolysis temperature and steam concentration on the reaction were also investigated. After 1.5 hours, the hydrolysis rate of CFC-12 was tested. The catalyst stability was analyzed after 30 hours.

## **water vapor concentration**

Electric heating sleeve as heating device to produce steam, firstly, clean and dry the glass sand tail gas absorption bottle and weigh it, record as m<sub>1</sub>. The second of, add a certain amount of water and carry out catalytic hydrolysis reaction, the reaction time was recorded as t. Finally, stop reacting and absorption bottle with water is weighed as m<sub>3</sub>, calculation of velocity, the formula is as follows

**See formula 1 in the supplemental files section.**

## **Analysis methods**

The qualitative and quantitative analysis of hydrolyzate was carried out by gas chromatography and mass spectrometry (Thermo Fisher GC-MS). MS detectors EI source and the electron energy is 70 eV. The hydrolysis rate of CFC-12 and formation rate of CO and CO<sub>2</sub> were calculated as follows:

$$[\text{hydrolysis rate of CFC-12}] = \frac{([\text{CFC-12}]_{\text{in}} - [\text{CFC-12}]_{\text{out}})}{[\text{CFC-12}]_{\text{in}}} \times 100\%$$

$$[\text{Yield of CO}_x] = \frac{[\text{CO}_x]_{\text{out}}}{([\text{CFC-12}]_{\text{in}} - [\text{CFC-12}]_{\text{out}})} \times 100\%$$

## Results And Discussion

### XRD patterns of MoO<sub>3</sub>/ ZrO<sub>2</sub>-TiO<sub>2</sub> calcined at different temperature

Fig.2 shows the component of the catalyst is mainly amorphous when calcination temperature is below 400 °C. As the temperature increasing, the morphology of MoO<sub>3</sub>/ ZrO<sub>2</sub>-TiO<sub>2</sub> crystal appeared. The corresponding characteristic diffraction peaks of tetragonal phase (Zr(MoO<sub>4</sub>)<sub>2</sub>) occurred with the 2θ of 23.180°, 30.526° and 50.033° at calcination temperature of 500 °C. The pattern shows crystal structure of anatase, it confirms the main constituents of the catalyst (MoO<sub>3</sub>/ ZrO<sub>2</sub>-TiO<sub>2</sub>) is tetragonal Zr (MoO<sub>4</sub>)<sub>2</sub> phase mixed with TiO<sub>2</sub> of anatase.

### XRD patterns of MoO<sub>3</sub>/TiO<sub>2</sub>-ZrO<sub>2</sub> at different calcination time

As shown in Fig.3, when the calcination time is 1 hour and 2 hours, the XRD patterns (MoO<sub>3</sub>/TiO<sub>2</sub>-ZrO<sub>2</sub>) indicate that the components are mainly amorphous with calcination temperature of 500 °C. When calcination time above 3 hours, the better crystal structures of MoO<sub>3</sub>/ZrO<sub>2</sub>-TiO<sub>2</sub> are observed in the XRD patterns.

### TEM patterns of MoO<sub>3</sub>/ZrO<sub>2</sub>-TiO<sub>2</sub> calcined at different temperature

It can be seen from the TEM diagram of MoO<sub>3</sub>/TiO<sub>2</sub>-ZrO<sub>2</sub>. When the calcination temperature is 400 °C, the catalyst mainly exists in amorphous state. With the increase of calcination temperature, the catalyst calcined at 500 °C mainly exists in crystalline phase. The selected area diffraction pattern in the lower right corner is concentric ring, which shows that the sample is polycrystalline, which is consistent with the XRD results. When the temperature continued to rise to 600 °C, the specific surface area and catalytic activity of the catalyst decreased, the main reason is the sintering of catalyst.

### BET N<sub>2</sub> adsorption and desorption patterns of MoO<sub>3</sub>/ZrO<sub>2</sub>-TiO<sub>2</sub> calcined at different temperature

As can be seen from table 1, with the increase of calcination temperature, the specific surface area of the catalyst decreases more sharply, which indicates that the catalyst has a certain degree of sintering. Combined with XRD, with the increase of calcination temperature, the intensity of diffraction peak

increased to a certain extent, and the specific surface area of catalyst calcined at 600 °C decreased 224.795 compared with that at 400 °C

**Table 1.** Specific surface area, average pore size and total pore volume of MoO<sub>3</sub>/ ZrO<sub>2</sub>-TiO<sub>2</sub>

	calcination temperature	specific surface area/m <sup>2</sup> ·g <sup>-1</sup>	Average pore size/nm	Total pore volume/cm <sup>3</sup> ·g <sup>-1</sup>
MoO <sub>3</sub> /ZrO <sub>2</sub> -TiO <sub>2</sub>	400°C	287.39	2.74	0.3978
	500°C	153.31	3.55	0.4447
	600°C	62.595	9.21	0.4115

It can be seen from the figure that the isotherm characteristics of all samples are concave to the relative pressure axis. The adsorption curve is not consistent with the desorption curve, that is, there is a hysteresis loop. The P/P<sub>0</sub> values of the catalysts calcined at 400 °C and 500 °C are 0.45- 0.99, which is a typical IV isotherm accompanied by H<sub>2</sub> hysteresis loop. The characteristics of these isotherms also reflect the formation of intergranular mesopores. The catalyst calcined at 600 °C is characterized by type IV isotherm and H<sub>1</sub> hysteresis loop, which is the result of homogeneous pore condensation. When the relative pressure is 0.75 and 0.9, the change slope of the isotherm is higher, which indicates that the mesoporous materials have better uniformity.

### NH<sub>3</sub>-TPD of MoO<sub>3</sub>/TiO<sub>2</sub>-ZrO<sub>2</sub> calcined at different temperatures

Temperature programmed desorption method uses pyridine, ammonia, 2,6-dimethylpyridine and tert Butyl Ammonium as adsorbents. Because of NH<sub>3</sub> have strong basicity (PK<sub>a</sub> = 9.2), high stability and small molecular volume, it's can be adsorbed on acid sites with different acid strength and easily enter into the pore channels of porous materials ,it is an ideal acid probe molecule. The peak temperature is often related to the acid strength, peak area and acid amount .The desorption temperatures of NH<sub>3</sub> were 100 °C ~150 °C, 200~230 °C and 500~700 °C, respectively, corresponding to the weak acid site desorption peak, medium strong acid site desorption peak and strong acid site desorption peak[21]. It can be seen from Fig. 6 that NH<sub>3</sub> has two strong acid sites (α and β) on MoO<sub>3</sub>/TiO<sub>2</sub>-ZrO<sub>2</sub>, the peak area is proportional to the amount of NH<sub>3</sub> adsorbed on the sample. That is, it is directly proportional to the amount of acid in the sample, the weak desorption peak of β indicates that the content of strong acid site is less, the α - desorption peak of MoO<sub>3</sub>/TiO<sub>2</sub>-ZrO<sub>2</sub> catalyst calcined at 500 °C was the strongest, indicating the highest content of weak acid. The results showed that the best hydrolysis effect of CFC-12 was obtained by MoO<sub>3</sub>/TiO<sub>2</sub>-ZrO<sub>2</sub> catalyst calcined at 500 °C, combined with the results of NH<sub>3</sub>-TPD characterization, the weak acid site of solid acid MoO<sub>3</sub>/TiO<sub>2</sub>-ZrO<sub>2</sub> has strong catalytic activity for the hydrolysis of CFC-12. The calcination temperature has a great influence on the acidity of the catalyst, the β - desorption peak of MoO<sub>3</sub>/TiO<sub>2</sub>-ZrO<sub>2</sub> catalyst calcined at 600 °C disappeared, the reason may be that higher calcination temperature is not conducive to the formation of medium strong acid sites.

## FT-IR of MoO<sub>3</sub>/TiO<sub>2</sub>-ZrO<sub>2</sub> calcined at different temperatures

Fig. 7 shows the FT-IR diagram at different calcination temperatures. It can be seen from the figure that the influence of calcination temperature on FT-IR diagram is great, the sample near 746 cm<sup>-1</sup> can be attributed to the vibration peak of Zr-O bond, 500-700 cm<sup>-1</sup> belongs to Ti-O vibration peak, near 990 cm<sup>-1</sup> is the stretching vibration absorption of Mo = O in crystalline MoO<sub>3</sub>. In addition, there are strong absorption peaks near 1631 cm<sup>-1</sup> and 3400 cm<sup>-1</sup>, 1631 cm<sup>-1</sup> is the bending vibration peak of -OH adsorbed by metal atoms on the surface of composite oxides, 3400 cm<sup>-1</sup> is the Strong absorption peak of stretching vibration of -OH. The absorption vibration peak of the catalyst calcined at 400 °C is weak, especially in the wavelet segment, the results show that the catalyst mainly exists in amorphous form and the results are consistent with those of XRD.

## Effect of MoO<sub>3</sub>/ZrO<sub>2</sub>-TiO<sub>2</sub> on the hydrolysis rate of CFC-12

### Effect of calcination temperature on the hydrolysis rate of CFC-12

It can be seen in Fig.8 that the hydrolysis rate increases with the increase of temperature from 300 °C to 500 °C, and decreases after 500 °C. The highly hydrolysis rate reaches 98.65 % at 500 °C. It is studied and analyzed that the occurrence of the catalyst is due to the temperature being too high, the catalyst is sintered, and the activity is lowered.

### Effect of calcination time on hydrolysis rate of CFC-12

Fig.9 is based on a previous study of the optimal calcination temperature. The effect of calcination time on the hydrolysis rate of CFC-12 at the optimum calcination temperature was investigated. The experimental results show that the catalytic hydrolysis rate of CFC-12 is up to 98.65% when the calcination time is 3 hours, When the calcination time is less than 3 hours, the calcination is incomplete and the structure is incomplete, so the hydrolysis rate is not too high. After calcination for 3 hours, the main structure of the solid acid catalyst MoO<sub>3</sub>/ZrO<sub>2</sub>-TiO<sub>2</sub> is tetragonal Zr (MoO<sub>4</sub>)<sub>2</sub> doped anatase TiO<sub>2</sub> structure. The hydrolysis rate decreased with the increase of calcination time, which is mainly due to the corrosion of the catalyst by HCl and HF produced by the hydrolysis of CFC-12 and calcination time is too long, the catalyst will be sintered, the dispersion of TiO<sub>2</sub> in ZrO<sub>2</sub> will be reduced, resulting in the specific surface area and activity of the catalyst will be reduced.

### Effect of catalytic hydrolysis temperature on the hydrolysis rate of CFC-12

Fig.10 shows that the hydrolysis rate of CFC-12 increases with the increase of catalytic hydrolysis temperature. The hydrolysis rate of CFC-12 reaches 98.65% at 400 °C, it remains unchanged after 400 °C. The rate of hydrolysis gradually increases due to the endothermic process of the reaction of CFC-12:  $\text{CF}_2\text{Cl}_2 + \text{H}_2\text{O} \rightarrow \text{CO}_2 + \text{HF} + \text{HCl}$ . According to the mass spectrum analysis, there is a certain amount of CO<sub>2</sub> in the hydrolysis products of CFC-12, which may be produced by the reaction of  $\text{CF}_2\text{Cl}_2 + \text{O}_2 + \text{H}_2\text{O} \rightarrow \text{CO}_2 + \text{HF} + \text{HCl}$ .

HCl, and the oxygen contained may come from dissolved oxygen in the air. The formation rate of  $\text{CO}_x$  ( $\text{CO}$  and  $\text{CO}_2$ ) are 72.44%, which may indicate that the catalytic hydrolysis of CFC-12 over  $\text{MoO}_3/\text{ZrO}_2\text{-TiO}_2$  is complete. All the above investigations indicate that the solid acid of  $\text{MoO}_3/\text{ZrO}_2\text{-TiO}_2$  composite with the calcination temperature of  $500^\circ\text{C}$  and calcination time of 3 hours in the catalytic hydrolysis of CFC-12 acts as an effective catalyst with high catalytic activity and selectivity. The solid acid catalyst  $\text{MoO}_3/\text{ZrO}_2\text{-TiO}_2$  prepared by calcining at  $500^\circ\text{C}$  for 3 hours is one of the ideal catalysts for catalytic hydrolysis of CFC-12.

### **The effect of water vapor concentration on the hydrolysis rate of CFC-12**

Fig.11 shows that water vapor concentration has a significant effect on the hydrolysis rate of CFC-12. In the absence of water vapor, the hydrolysis of CFC-12 was 14.31%. The hydrolysis rate of CFC-12 increased with the increase of steam concentration, and decreases after 83.18%. When the steam concentration was 83.18%, the hydrolysis rate reached the maximum value of 98.65%. The hydrolysis rate decreased with the further increase of steam concentration. The main reason is that the reaction rate is accelerated and the gas-solid contact time is shortened with the increase of water vapor concentration, as well as the lower reaction temperature as more water vapor is involved in the system. It is concluded that the optimum volume fraction of water vapor is 83.18%.

### **The effect of reaction time on the hydrolysis rate of CFC-12**

As shown in Figure 12, when the reaction time is less than 10 hours, the hydrolysis rate of CFC-12 is more than 98.00%, indicating that the solid acid of  $\text{MoO}_3/\text{ZrO}_2\text{-TiO}_2$  catalyst has good thermal stability. The hydrolysis rate of CFC-12 drops from 98.00% to 65.34% as the reaction time reaches 20 hours. When the reaction time exceeds 20 hours, the hydrolysis rate decreased slowly. All of the above studies show that the solid acid of  $\text{MoO}_3/\text{ZrO}_2\text{-TiO}_2$  composite with the calcination temperature of  $500^\circ\text{C}$  and calcination time of 3 hours in the catalytic hydrolysis of CFC-12 has high thermal stability.

## **$\text{MoO}_3/\text{TiO}_2\text{-ZrO}_2$ SEM diagram of the reaction before and after**

The SEM images of  $\text{MoO}_3/\text{ZrO}_2\text{-TiO}_2$  composite before and after the catalytic hydrolysis reaction of CFC-12 were given in Fig.13. The  $\text{MoO}_3/\text{ZrO}_2\text{-TiO}_2$  composite is the shape of lumpy, and has a good crystal structure with calcination temperature of  $500^\circ\text{C}$  and calcination time of 3 hours, which is consistent with the XRD results. In addition to the complete crystal form, amorphous particles appear after the reaction, mainly due to the introduction of  $\text{SiO}_2$ , which indicates that  $\text{MoO}_3/\text{ZrO}_2\text{-TiO}_2$  catalyst has high stability and long service life.

## **Characterization of $\text{MoO}_3/\text{TiO}_2\text{-ZrO}_2$ EDS after reaction**

The EDS diagram showed that no fluorine(F) was detected after the reaction, indicating that fluorine products did not participate in the reaction, and elemental carbon(C) appeared mainly due to the introduction of conductive adhesive in the test. The results show that  $\text{MoO}_3/\text{ZrO}_2\text{-TiO}_2$  catalyst has high selectivity and stability.

## Conclusions

The results show that the hydrolysis rate of CFC-12 is more than 98.00%, and the optimum conditions of catalyst dosage, flow rate, water vapor volume fraction and hydrolysis temperature are 1.00 g, 1 mL/min, 83.18% and 400°C, respectively. The main hydrolysis products were CO, CO<sub>2</sub>, HF and HCl. The main constituents of the catalyst ( $\text{MoO}_3/\text{ZrO}_2\text{-TiO}_2$ ) is tetragonal  $\text{Zr}(\text{MoO}_4)_2$  phase catalyst showing higher activity and selectivity. When the reaction time overtook 30 hours, hydrolysis rate of CFC-12 still remained over 65.00%, showing that the catalyst has high stability. In short,  $\text{MoO}_3/\text{TiO}_2\text{-ZrO}_2$  is a promising catalyst for the catalytic hydrolysis of CFC-12.

## Declarations

## Ethics approval and consent to participate

Not applicable

## Consent to publish

Not applicable

## Availability of data and materials

All data generated or analyzed during this study are included in this manuscript

## Competing interests

The authors declare that they have no competing interests.

## Funding

This work was funded by the National Natural Science Fund(51568068)

**Authors' Contributions** *Zhiqian Li, Tong Zhou, Guoqing Ren and Xiaofang Tan* conceived and designed the experiments; *Zhiqian Li and Guoqing Ren* performed the experiments; *Zhiqian Li and Tong Zhou* analyzed the data; *Zhiqian Li, Tong Zhou, and Guoqing Ren* wrote and modified the paper. All authors read and approved the final manuscript.

## Acknowledgement

This work was funded by the National Natural Science Fund (51568068), Yunnan Minzu University is gratefully acknowledged for providing us with the facilities for the XRD and BET study. At the same time, I would like to thank Tong Zhou, Guoqing Ren, Xiaofang Tan for their help with the experiment and Professor Tiancheng Liu guidance to the experiment; *Zhiqian Li and Tong Zhou* analyzed the data; *Zhiqian Li, Tong Zhou, and Guoqing Ren* wrote and modified the paper. All authors read and approved the final manuscript.

### Authors' Information

<sup>1</sup> *College of Chemistry and Environment, Yunnan Minzu University, Joint Research Centre for International Cross-border Ethnic Regions Biomass Clean Utilization in Yunnan, Kunming 650500, China*

<sup>2</sup> *Dehong teachers college, Yunnan, Dehong 678400, China*

## Abbreviations

CFC-12: Difluorodichloromethane

CFCs: Chlorofluorocarbons

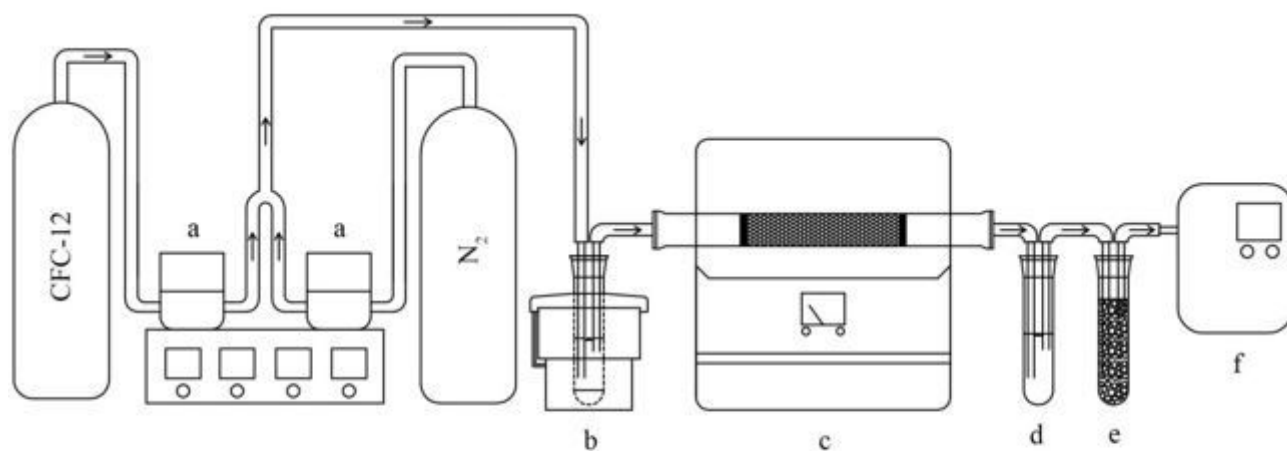
## References

1. Molina MJ, Rowland FS (1974) Stratospheric sink for chlorofluoromethanes: chlorine atom-catalysed destruction of ozone[J]. *Nature*, 249: 810-812.
2. Roland FS, Molina MJ (1994) Ozone Depletion-20 Years After the Alarm[J]. *Chemical & Engineering News*, 72: 8-13.
3. Gammie F (1995) Breakaway iceberg 'due to warming'[J]. *Nature International Weekly Journal of Science*, 374:108-108.
4. Guohong D, Yue Z, Changlin L, Yong Y, Zhengchao L, Huiqi H (1997) Decomposition of gaseous CF<sub>2</sub>ClBr by cold plasma method[J]. *J. Environ. Sci (in Chinese)*, 9: 11-19.

5. Wenboi LZPXD, Huiqi H, Jian ZZH (1997) Decomposition of  $\text{CF}_3\text{Cl}$  by corona discharge [J]. *Envir O.Sei.* 1997:95-99.
6. Gal' A, Ogata A, Futamura S, Mizuno K (2003) Mechanism of the dissociation of chlorofluorocarbons during nonthermal plasma processing in nitrogen at atmospheric pressure[J]. *The Journal of Physical Chemistry A*, 107: 8859-8866.
7. Ya-fen W, Wen-jhy L, Chuh-yung C, Lien-te H (1999) Decomposition of CFC-12 by adding hydrogen in a cold plasma system[J]. *Environmental science & technology*,33: 2234-2240.
8. Tiancheng L, Ping N, Hongbing W, Hong G, Linzhuan M (2010) Catalytic Decomposition of CFC-12 (CFC-12) Over Solid Super Acid  $\text{MoO}_3/\text{ZrO}_2$ [J]. *Asian Journal of Chemistry (in chinese)*, 22: 4431-4438.
9. Ma Z Hua W, Tang Y(2000)Catalytic decomposition of CFC-12 over solid acids  $\text{WO}_3/\text{M}_x\text{O}_y$ ( $\text{M}=\text{Ti, Sn, Fe}$ )[J]. *Journal of Molecular. Catalysis A: Chemical*,159: 335-345.
10. Weiming H, Feng Z, Zhen M, Yi T, Zi G (2000)  $\text{WO}_3/\text{ZrO}_2$  Strong Acid as a Catalyst for the Decomposition of Chlorofluorocarbon (CFC-12) [J]. *Chemical Research in Chinese Universities*,16: 185-187.
11. Takita Y, Moriyama JI, Yoshinaga Y, Nishiguchi H, Ishihara T, Yasuda S, Ueda Y, Kubo M, Miyamoto A (2004) Adsorption of water vapor on the  $\text{AlPO}_4$ -based catalysts and reaction mechanism for CFCs decomposition[J]. *Applied Catalysis A: General*,271: 55-60.
12. Ma Z, Hua W, Tang Y, Gao Z (2000) Catalytic decomposition of CFC-12 over solid acids  $\text{WO}_3/\text{M}_x\text{O}_y$ ( $\text{M}=\text{Ti, Sn, Fe}$ )[J]. *Journal of Molecular. Catalysis A: Chemical*, 159: 335-345.
13. Hongxia Zhang, Ching FN, SukYL (2005) Catalytic decomposition of chlorodifluoromethane (HCFC-22) over platinum supported on  $\text{TiO}_2\text{-ZrO}_2$  mixed oxides[J]. *Applied Catalysis B: Environmental*,55: 301-307.
14. Navio J A, Macías M, Colón G, Snchez-Soto PJ, Augugliaro V, Palmisano L (1994) et al. Combined use of XPS, IR and EDAX techniques for the characterization of  $\text{ZrO}_2\text{-SiO}_2$  powders prepared by a sol-gel process[J]. *Applied surface science*, 81: 325-329.
15. Devotta S, Waghmare A V, Sawant N N (2001) Alternatives to HCFC-22 for air conditioners[J]. *Applied Thermal Engineering*, 21: 703-715.
16. Zuiderweg A, Kaiser J, Laube JC (2012) Stable carbon isotope fractionation in the UV photolysis of CFC-11 and CFC-12[J]. *Atmospheric chemistry and physics*,12: 4379-4385.
17. Suk YL, Hongxia Z, Ching FN (2004) Deactivation of gold catalysts supported on sulfated  $\text{TiO}_2\text{-ZrO}_2$  mixed oxides for CO oxidation during catalytic decomposition of chlorodifluoromethane (HCFC-22) [J]. *Catalysis letters*,92: 107-114.
18. Wang I, Chang WF, Shiao RJ (1983) Nonoxidative dehydrogenation of ethylbenzene over  $\text{TiO}_2\text{-ZrO}_2$  catalysts: I. Effect of composition on surface properties and catalytic activities[J]. *Journal of Catalysis*,83: 428-436.

19. Vishwanathan V, Roh HS, Kim JW, Jun KW (2004) Surface properties and catalytic activity of  $\text{TiO}_2$ - $\text{ZrO}_2$  mixed oxides in dehydration of methanol to dimethyl ether[J]. Catalysis letters,96: 23-28.
20. Zhen M, Weiming H, Yi T, Zi G (1999) Catalytic Decomposition of CFC-12 over  $\text{WO}_3/\text{TiO}_2$ [J]. Chemistry Letters, 1215-1216.
21. Chary KVR, Bhaskar TK, Gurram R, Kondakindi R (2001) Characterization and reactivity of molybdenum oxide catalysts supported on niobia[J]. Physical Chemistry B,19: 4392-4399

## Figures



a: mass flowmeter b: water vapor generating c: tube furnace d: NaOH adsorption e: desiccant

f: GC-MS

Figure 1

Flow diagram of CFC-12 catalytic hydrolysis experiment

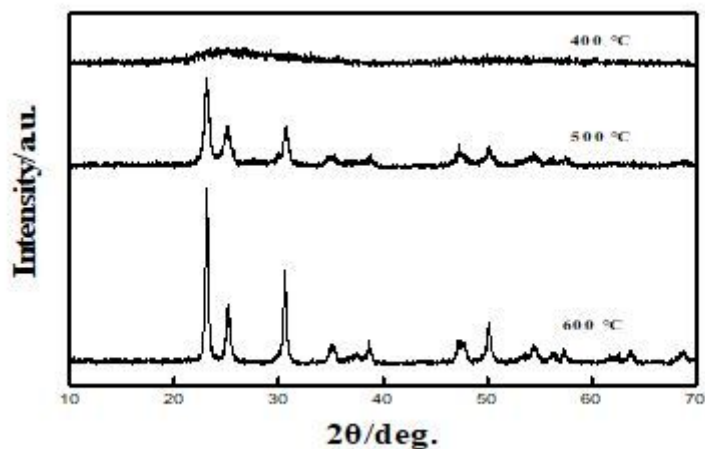


**Figure 2**

XRD patterns of MoO<sub>3</sub>/ ZrO<sub>2</sub>-TiO<sub>2</sub> calcined at different temperatures

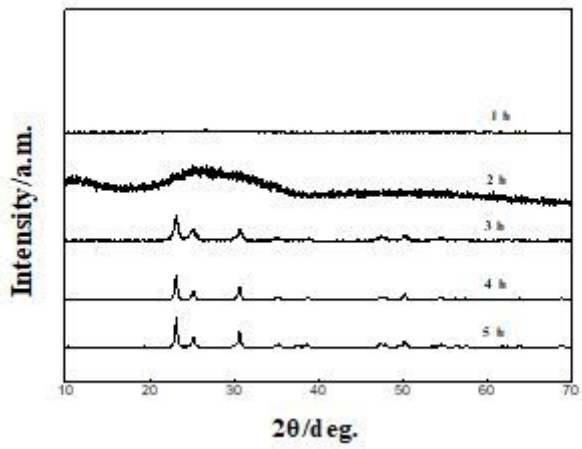


**Figure 3**

XRD patterns of MoO<sub>3</sub>/TiO<sub>2</sub>-ZrO<sub>2</sub> at different calcined time

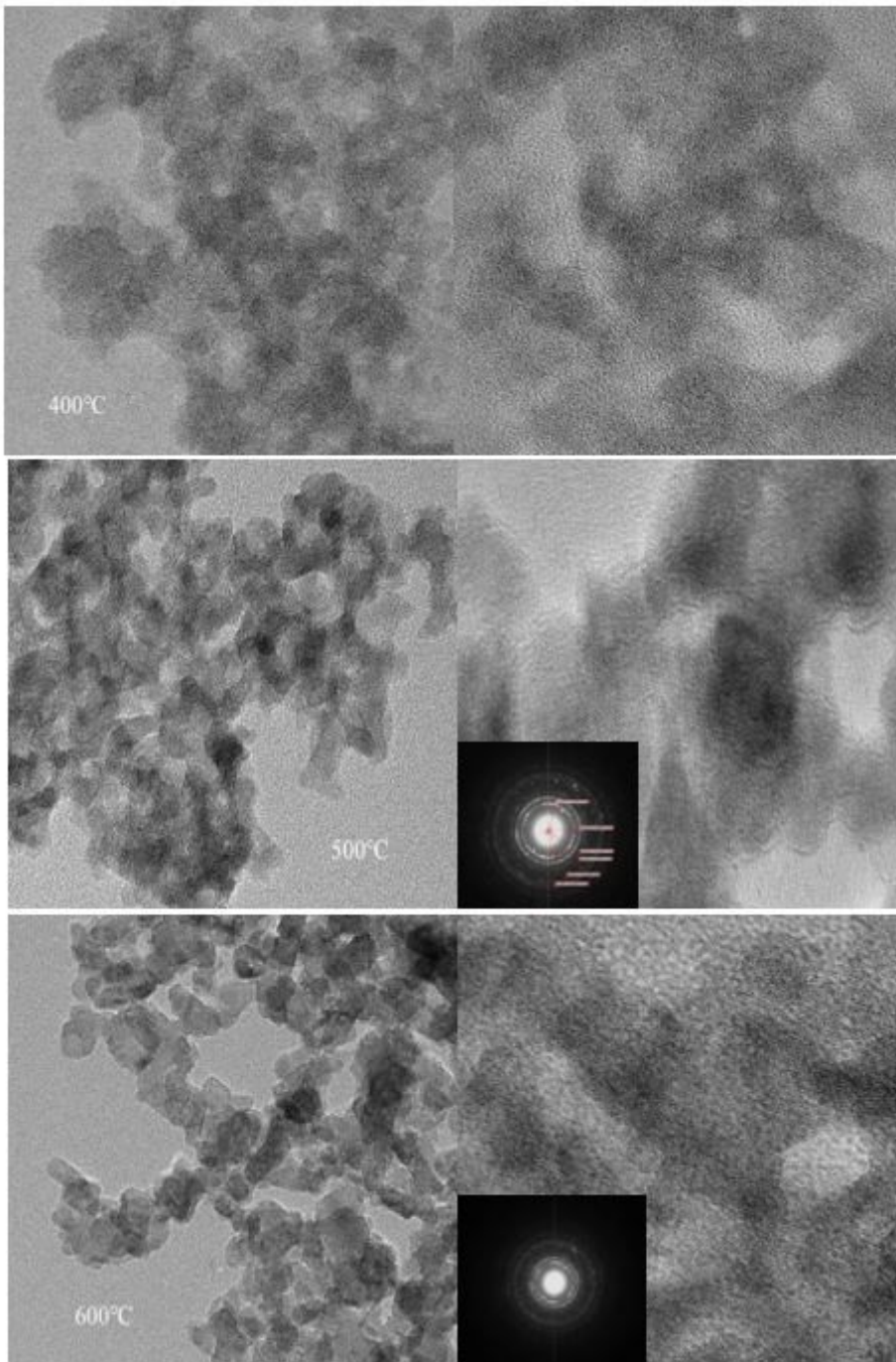


**Figure 4**

TEM patterns of  $\text{MoO}_3/\text{ZrO}_2\text{-TiO}_2$  calcined at different temperature

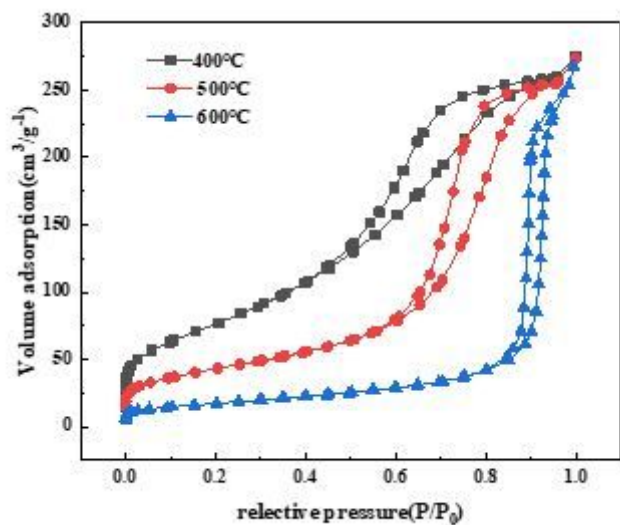


Figure 5

N<sub>2</sub> adsorption and desorption of MoO<sub>3</sub>/ ZrO<sub>2</sub>-TiO<sub>2</sub> calcined at different temperature

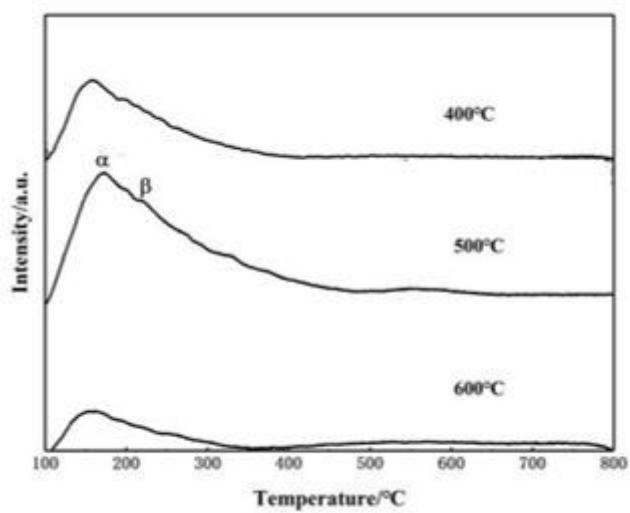


Figure 6

NH<sub>3</sub>-TPD of MoO<sub>3</sub>/TiO<sub>2</sub>-ZrO<sub>2</sub> calcined at different temperatures

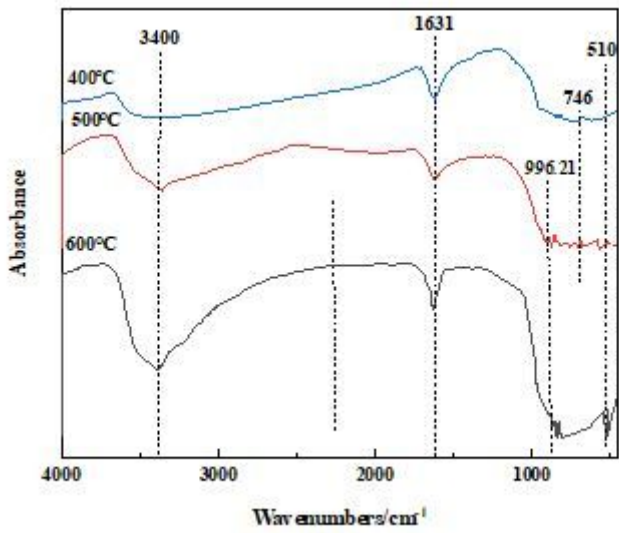


Figure 7

FT-IR of MoO<sub>3</sub>/TiO<sub>2</sub>-ZrO<sub>2</sub> calcined at different temperatures

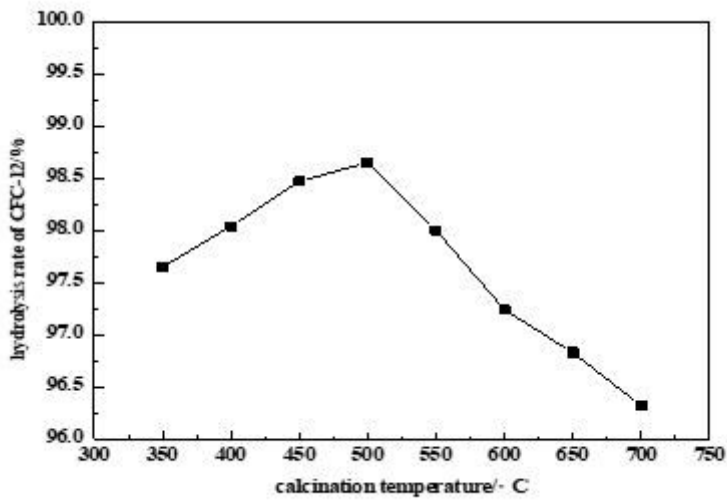


Figure 8

Effect of Calcination Temperature on CFC-12 hydrolysis Rate

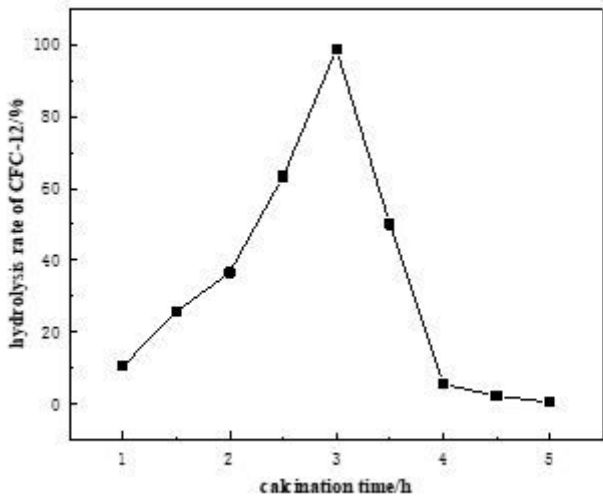


Figure 9

Effect of calcination time on hydrolysis rate of CFC-12

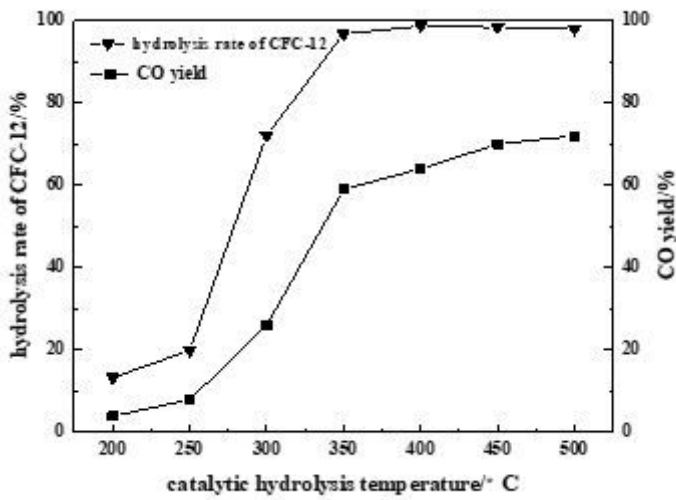


Figure 10

Effect of catalytic hydrolysis temperature on hydrolysis rate of CFC-12

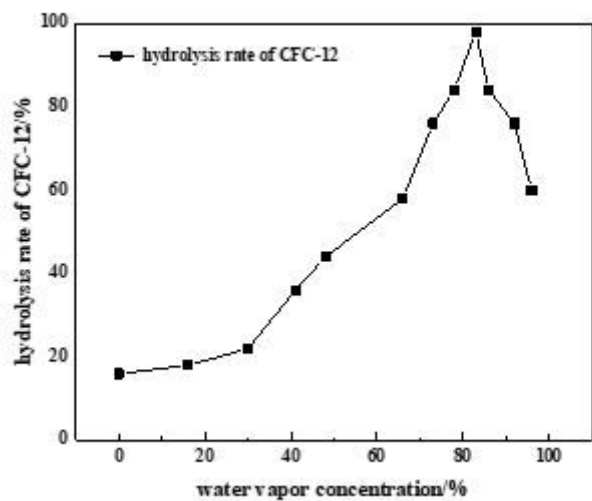


Figure 11

The effect of water vapor concentration on the CFC-12 hydrolysis

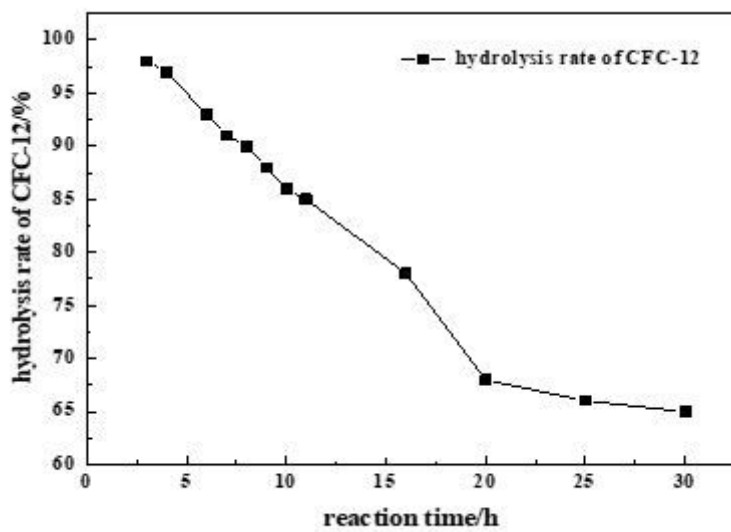


Figure 12

The effect of reaction time on the CFC-12 hydrolysis

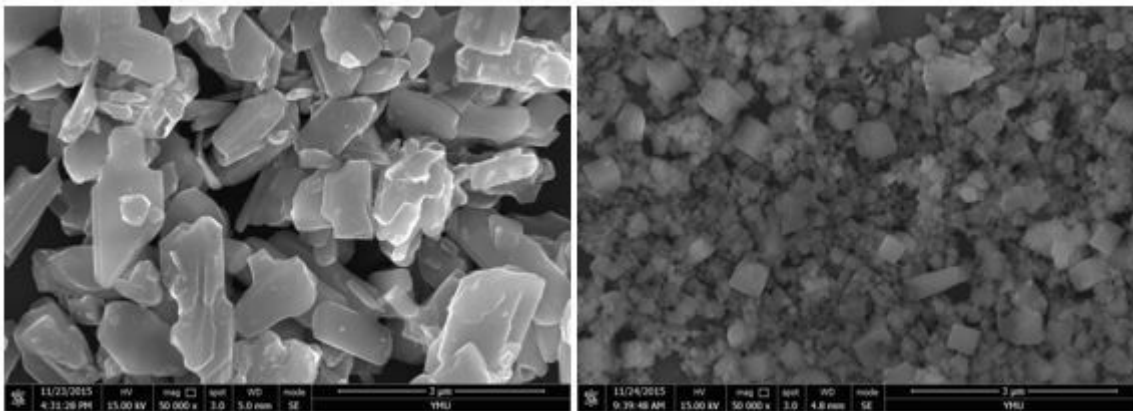


Figure 13

MoO<sub>3</sub>/TiO<sub>2</sub>-ZrO<sub>2</sub> SEM diagram of the reaction before and after

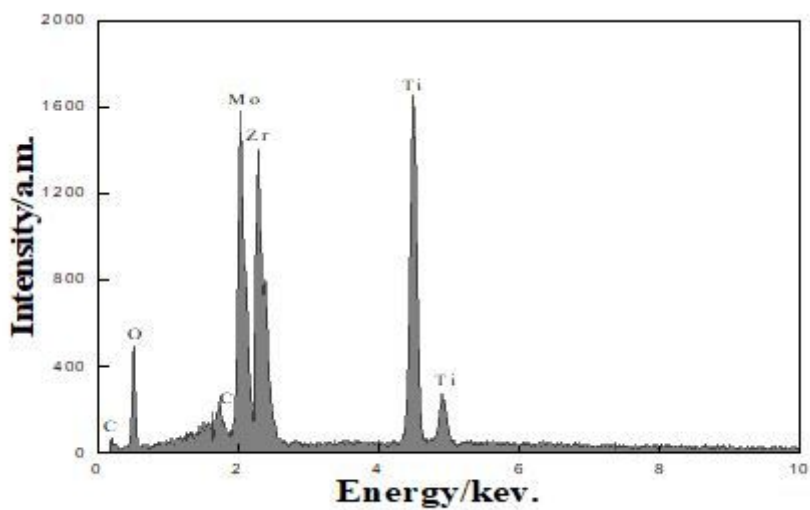


Figure 14

Characterization of MoO<sub>3</sub>/TiO<sub>2</sub>-ZrO<sub>2</sub> EDS after reaction

## Supplementary Files

This is a list of supplementary files associated with this preprint. Click to download.

- [formula.docx](#)